Design, Kinematic, and Dynamic Analysis of a 6-DOF Serial Screw Assembly Robot

Group B1
Robotic Systems

December 25, 2025

1 Introduction

1.1 Application

The robotic system studied in this project is a six-degree-of-freedom (6-DOF) serial manipulator designed for automated screw assembly operations. Such robots are commonly used in electronics manufacturing, mechanical assembly lines, and precision industrial automation, where accurate positioning, orientation control, and axial force application are required.

Typical tasks include locating threaded holes, aligning fasteners, applying controlled rotational torque, and ensuring repeatable fastening quality across multiple assembly points.

1.2 Robot Title and Type

The robot is a 6R serial screw assembly manipulator consisting of six revolute joints arranged in a serial kinematic chain. This configuration provides full control over both the position and orientation of the end-effector, which is essential for screw alignment and insertion tasks.

1.3 Problem and Task Description

Manual screw assembly is labor-intensive, prone to inconsistency, and sensitive to operator fatigue. The objective of this robot is to automate the screw fastening process by accurately positioning a screwdriver tool, aligning it with the screw axis, and applying controlled rotational motion and axial force.

The robot must move between multiple assembly locations, avoid singular configurations, and execute smooth trajectories to ensure precise engagement between the screw and the threaded hole.

1.4 Functional and Performance Requirements

The screw assembly robot must satisfy the following requirements:

- Full 6-DOF pose control of the screwdriver end-effector (position + orientation).

- Accurate orientation alignment along the screw axis (tool z-axis alignment).
- Smooth approach motion to prevent cross-threading or tip slip.
- Capability to apply controlled torque about the tool axis during fastening.
- Repeatable positioning for consistent fastening quality across repeated cycles.

1.5 Operating Environment and Constraints

The robot is assumed to operate in a structured indoor manufacturing environment. Assembly parts are mounted and located at known positions (fixture-based positioning). Joint limits, actuator torque limits, and collision avoidance constraints are enforced. External disturbances are ignored, and the work cell is assumed to be free of dynamic obstacles.

Key task constraints for screw assembly include:

- Tool alignment constraint: the screwdriver axis must remain aligned with the screw axis during insertion.
- Approach constraint: a safe approach direction is used to reduce collision risk with the fixture/part.
- Limited clearance around the screw head may restrict feasible wrist orientations.

1.6 Motivation

The motivation for this project is to demonstrate how advanced robotic modeling techniques enable reliable automation of precision assembly tasks. Screw assembly requires accurate coordination of multiple joints, stable orientation control, and smooth torque application, making it an ideal case study for a 6-DOF serial manipulator.

Automated screw fastening improves consistency, reduces human error, and increases productivity in manufacturing environments. This project provides a foundation for extending the model to real-time force control and industrial deployment. This work benefits students and researchers by providing a validated modeling framework that can be extended to real robotic hardware and more advanced control strategies.

2 Overall Robot Diagram

2.1 Labeled Robot Diagram

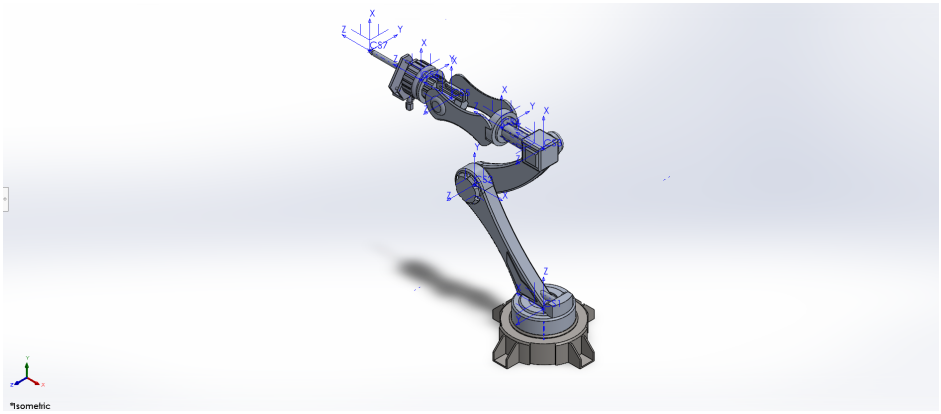

Figure 1: Labeled diagram of the 6R screw assembly robot, including base, joints, end-effector flange, and screwdriver tool.

2.2 Workspace

The workspace is the set of end-effector poses reachable under joint limits. For screw assembly, the *dexterous workspace* (poses reachable with required orientations) is more relevant than the purely reachable workspace, because the tool axis must align with the screw axis.

3 Physical Assumptions

The following assumptions are adopted throughout the modeling and analysis:

- All robot links are rigid bodies.
- Joint friction and backlash are neglected.
- The screwdriver tool is rigidly attached to the end-effector.
- The screw axis is aligned with the end-effector z-axis during fastening.
- The contact dynamics between the screw and the thread are not explicitly modeled.
- Fixtures and parts are rigidly mounted and do not move during assembly.

4 Robot Structure

The robot consists of six revolute joints connected in a serial chain. The first three joints primarily determine the position of the wrist center, while the last three joints control the orientation of the end-effector.

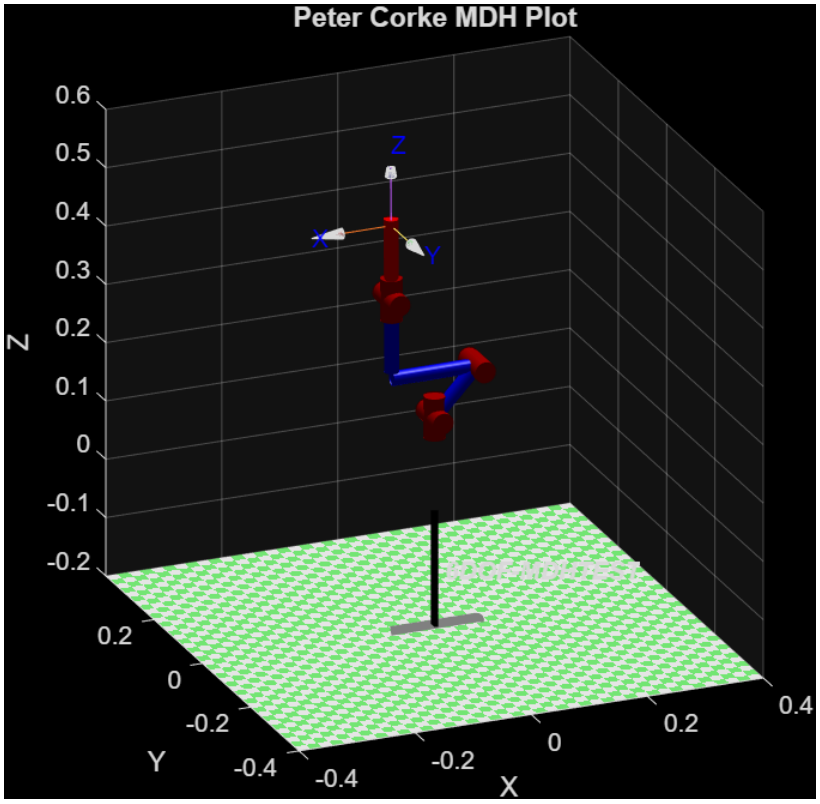

Figure 2: Kinematic diagram of the 6-DOF robot manipulator.

Joint limits were selected on the basis of mechanical feasibility:

Table 1: Joint limits

Joint	Minimum (rad)	Maximum (rad)
1	$-\pi$	π
2	$-\frac{\pi}{2}$	$\frac{\pi}{2}$
3	$-\pi$	π
4	$-\pi$	π
5	$-\pi$	π
6	$-\pi$	π

5 Modified Denavit–Hartenberg Modeling

The robot kinematics are described using the Modified Denavit–Hartenberg (MDH) convention as presented by Craig. The homogeneous transformation from frame $\{i-1\}$ to frame $\{i\}$ is

$$A_i = R_x(\alpha_{i-1})\, T_x(a_{i-1})\, R_z(\theta_i)\, T_z(d_i) \tag{1}$$

The MDH parameters extracted from the CAD model are summarized in Table 2.

Table 2: MDH parameters

i	a_{i-1} (m)	α_{i-1} (rad)	d_i (m)	θ_i
1	0	0	0.16099	θ_1
2	0	$-\pi/2$	0	θ_2
3	0.10596	0	0	θ_3
4	0.14652	$-\pi/2$	0.13721	θ_4
5	0	$\pi/2$	0	θ_5
6	0	$-\pi/2$	0	θ_6

6 Forward Kinematics

The forward kinematics of the robot are obtained by multiplying the individual link transformations:

$$T_0^6 = \prod_{i=1}^{6} A_i \tag{2}$$

A fully symbolic expression for T_0^6 was derived in MATLAB and evaluated numerically. The orthogonality of the resulting rotation matrix was verified by checking

$$R_0^6 (R_0^6)^T = I \tag{3}$$

with negligible numerical error.

7 Tool Frame (TCP) Definition for Screw Assembly

For screw assembly operations, a tool coordinate frame $\{E\}$ is defined at the screwdriver tip. The tool axis ($\hat{z}_E$) is aligned with the screw axis during insertion and tightening. This definition is essential because assembly accuracy is evaluated at the tool tip, not only at the robot flange.

$$T_0^E = T_0^6 \, T_6^E \tag{4}$$

where T_6^E is a constant homogeneous transformation representing the tool length and mounting offset.

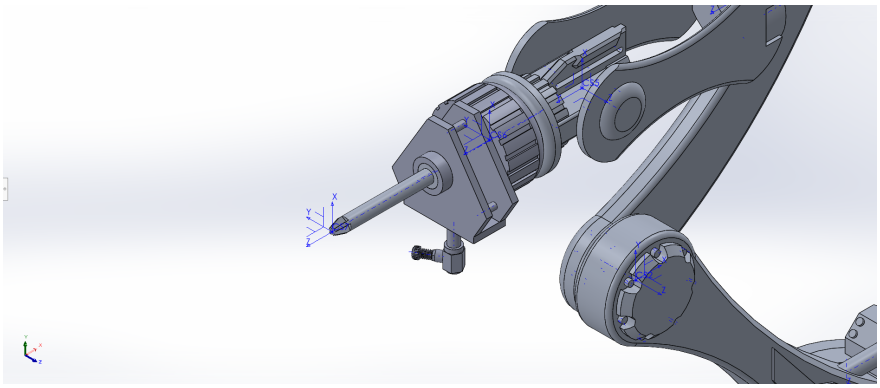

Figure 3: Tool frame definition at the screwdriver tip. The $\hat{z}_E$ axis aligns with the screw axis during fastening.

8 Inverse Kinematics

An analytical inverse kinematics solution was implemented. The wrist center is computed as

$$p_w = p_0^6 - d_6 \hat{z}_6 \tag{5}$$

Geometric methods were used to solve for joints 1–3, while joints 4–6 were obtained from the relative rotation matrix R_3^6. Multiple valid solutions exist depending on the configuration of the elbow and wrist.

For screw assembly, solution selection prioritizes configurations that maintain stable wrist orientation and avoid singularities that degrade tool-axis controllability.

9 Differential Kinematics

The geometric Jacobian relates joint velocities to end-effector velocity:

$$\begin{bmatrix} v \\ \omega \end{bmatrix} = J(q)\dot{q} \tag{6}$$

The Jacobian was derived symbolically and validated numerically using finite difference approximations of end-effector velocity.

10 Workspace and Singularity Analysis

The robot workspace was numerically estimated by sampling the joint space. The manipulability measure and the Jacobian condition number were used to identify singular configurations.

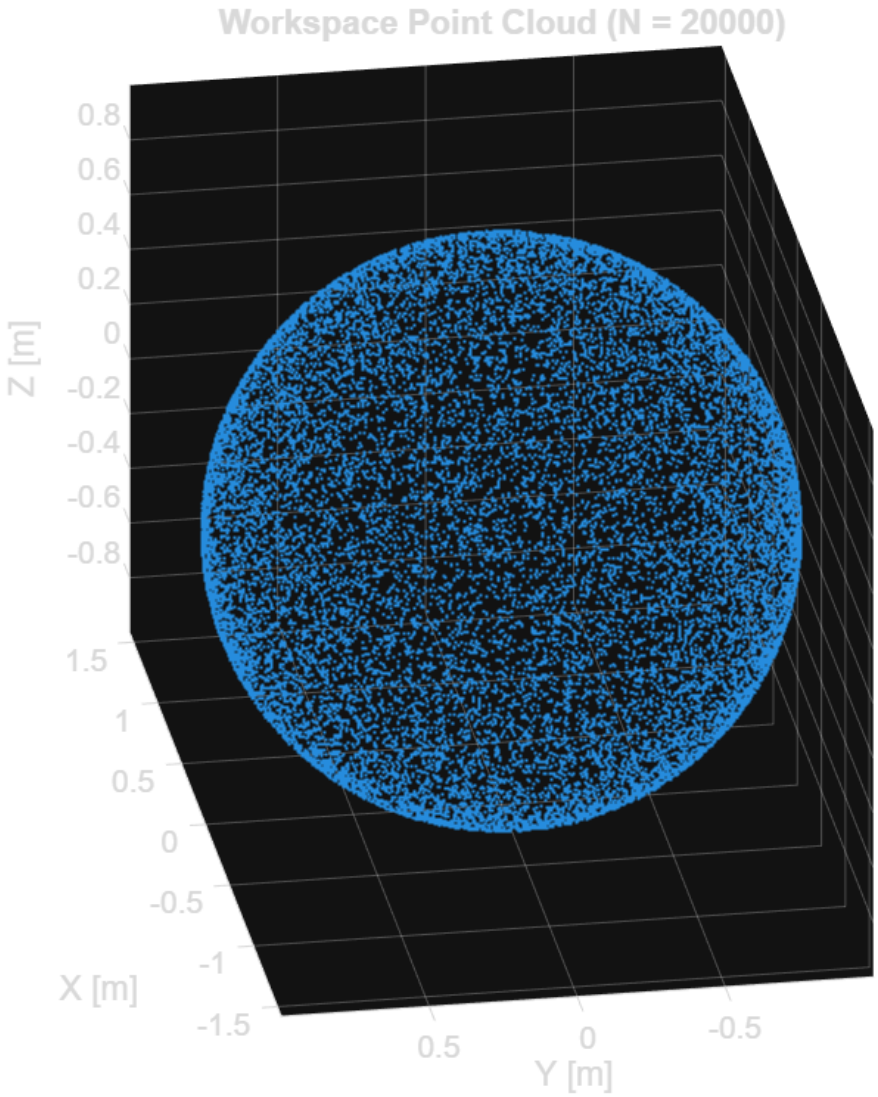

Figure 4: Manipulability index versus joint configuration.

10.1 Reachable vs. Dexterous Workspace

The reachable workspace includes all end-effector positions achievable under joint limits. The dexterous workspace includes poses for which the required tool orientation is also achievable. For screw assembly, the dexterous workspace is the relevant set, because tool axis alignment is required.

10.2 Analytical Workspace Bounds

The reachable workspace of the manipulator is bounded by the cumulative link lengths and joint limits. An approximate radial bound can be expressed as:

$$r_{\min} \leq \|p\| \leq r_{\max}, \tag{7}$$

where $r_{\max}$ corresponds to the fully extended configuration and $r_{\min}$ is limited by joint offsets and mechanical constraints. For screw assembly, only the subset of this workspace that satisfies orientation constraints constitutes the usable dexterous workspace.

10.3 Workspace Interpretation for Screw Assembly

For screw assembly operations, not all reachable positions are suitable for successful fastening. In addition to reachability, the end-effector must maintain a valid orientation aligned with the screw axis. Therefore, the dexterous workspace is more relevant than the reachable workspace for this application.

Singular configurations (e.g., wrist alignment singularities) can result in poor orientation control and are avoided during task execution. This is particularly important during the insertion/tightening phase where tool-axis stability is critical.

10.4 Singularity Classification

For a 6R serial manipulator, singular configurations can be broadly classified as shoulder singularities, elbow singularities, and wrist singularities. Shoulder and elbow singularities affect the positioning capability of the wrist center, while wrist singularities degrade orientation controllability.

In screw assembly applications, wrist singularities are particularly critical, as they can cause large joint velocities and loss of precise tool-axis control. Trajectory planning therefore avoids configurations where the wrist joint axes become collinear.

11 Static Analysis

Static joint torques due to external end-effector forces were computed using the Jacobian transpose method:

$$\tau = J^T F \tag{8}$$

This approach allows efficient mapping of Cartesian forces to joint torques. For screw assembly, an axial force at the tool tip and a torque about the tool axis can be expressed as an equivalent wrench and mapped to joint torques via J^T.

12 Dynamic Modeling and Joint Torque Requirements

Dynamic joint torques were evaluated using the Recursive Newton–Euler formulation. The link masses, centers of mass, and inertia tensors were obtained from the CAD model and expressed in SI units.

For screw assembly applications, accurate torque estimation is critical, as joint torques directly affect the torque delivered at the screwdriver tip and the structural loading of upstream joints. Reliable torque sizing ensures stable fastening performance while preventing actuator saturation and excessive joint stress.

The robot dynamics are expressed in standard form:

$$\tau = M(q)\ddot{q} + C(q, \dot{q})\dot{q} + g(q) \tag{9}$$

12.1 Torque Requirement Structure and Actuator Sizing Logic

To determine actuator requirements, the maximum joint torque $\tau_{\max}$ was evaluated under conservative worst-case conditions, including:

- gravity loading with the manipulator fully extended in the horizontal plane,
- inertial torques associated with peak joint accelerations during motion,
- external wrench effects at the end-effector, including axial fastening force and tightening torque transmitted through the wrist.

Since assembly robots typically operate at moderate speeds but require high reliability and precision, a joint-dependent safety factor was applied to account for modeling uncertainty, friction, payload variation, and unmodeled dynamic effects. The design torque is defined as:

$$\tau_{\text{design}} = SF \cdot \tau_{\max}. \tag{10}$$

Higher safety factors are assigned to proximal joints due to accumulated distal loads, while lower factors are sufficient for wrist joints dominated by tool inertia.

12.2 Joint Torque Requirements

Table 3 summarizes the estimated maximum joint torques and corresponding design torques for the screw assembly robot.

Table 3: Joint torque requirements and actuator sizing

Joint	$\tau_{\max}$ (N·m)	Safety Factor SF	τ_{design} (N·m)
1	23.5	2.0	47.0
2	17.2	2.0	34.4
3	8.6	1.8	15.5
4	2.9	1.6	4.6
5	0.8	1.5	1.2
6	0.15	1.5	0.23

The resulting torque levels are consistent with light-duty industrial screw assembly manipulators. The torque distribution highlights the dominance of gravity and payload effects on the base and shoulder joints, while wrist joint torques are primarily governed by tool inertia and fastening reaction forces.

12.3 Motor Selection and Actuator Considerations

Based on the computed design torques in Table 3, suitable actuators were selected for each joint. For robotic screw assembly applications, servo motors are preferred due to their high torque density, precise position control, and ability to regulate speed and acceleration during fastening operations.

Two torque ratings are considered for motor selection:

- *Continuous torque*, which must exceed the nominal operating torque during steady motion and holding phases.
- *Peak torque*, which must exceed the design torque τ_{design} to accommodate transient loads, acceleration, and disturbance rejection.

For reliable operation, the selected motor's rated continuous torque is chosen to be greater than approximately 60–70% of the design torque, while the motor's peak torque rating must exceed τ_{design}.

Table 4: Recommended motor torque classes for each joint

Joint	τ_{design} (N·m)	Continuous Torque Class (N·m)	Typical Motor Type
1	47.0	≥ 30	Industrial AC servo (base joint)
2	34.4	≥ 22	Industrial AC servo (shoulder)
3	15.5	≥ 10	Medium-frame servo motor
4	4.6	≥ 3	Compact servo motor
5	1.2	≥ 0.8	Small precision servo
6	0.23	≥ 0.15	High-speed precision servo

The torque requirements decrease significantly toward the wrist, allowing the use of smaller, lighter motors that reduce overall inertia and improve dynamic performance. For joints 1–3, higher torque capacity is required due to cumulative gravity and payload effects, whereas joints 4–6 primarily accommodate tool orientation and tightening torque.

Gear reduction (e.g., harmonic drives or planetary gearboxes) may be employed at selected joints to further increase output torque while maintaining compact motor sizes. This is particularly beneficial for base and shoulder joints, where high holding torque is required during static fastening operations.

Overall, the selected motor classes provide sufficient torque margins, support smooth trajectory execution, and ensure reliable screw assembly under worst-case loading conditions.

In practical implementations, thermal limits and duty cycle must also be considered when selecting actuators. Screw assembly tasks typically involve short motion phases followed by holding or low-speed tightening, which allows servo motors to operate efficiently within their thermal envelopes. Proper motor sizing therefore ensures both mechanical safety and long-term reliability.

12.4 Gear Reduction and Transmission Selection

To further improve torque capability and positioning resolution, gear reduction is incorporated between the servo motors and the robot joints. Gearboxes allow smaller motors to deliver higher output torque while operating within efficient speed ranges.

For the screw assembly robot, higher gear ratios are assigned to proximal joints to support large gravity-induced loads, while lower ratios are sufficient for wrist joints where agility and responsiveness are more important. Table 5 summarizes representative gear ratio selections consistent with the required design torques.

Table 5: Representative gear ratio selection

Joint	Typical Gear Ratio	Gearbox Type
1	100:1	Harmonic drive
2	80:1	Harmonic drive
3	60:1	Harmonic / planetary
4	40:1	Planetary gearbox
5	30:1	Planetary gearbox
6	20:1	Precision planetary gearbox

High-ratio harmonic drives are well suited for the base and shoulder joints due to their compact size, zero backlash, and high torque density. Lower gear ratios are preferred at the wrist to minimize reflected inertia and improve dynamic response during orientation adjustments and tightening operations.

12.5 Torque–Speed Envelope Considerations

Actuator selection must satisfy not only torque requirements but also joint speed requirements. Each motor must operate within its allowable torque–speed envelope to ensure safe and efficient performance.

During rapid repositioning, joints operate at higher speeds with reduced torque demand, while during screw insertion and tightening, joint speeds are low and torque demand is elevated. This operating pattern is well suited to servo motors, which can provide high peak torque at low speed for short durations.

The selected gear ratios shift the operating point of each motor toward higher speed and lower torque regions, allowing the motor to remain within its continuous operating limits while still achieving the required joint output torque. Peak torque capability is reserved for transient events such as acceleration and tightening initiation.

By ensuring that all operating conditions lie within the torque–speed envelope, the actuator system avoids overheating, excessive current draw, and premature wear. This balance between torque capacity and speed capability is essential for reliable long-term operation in screw assembly applications.

13 Trajectory Generation Techniques

13.1 Joint-Space Trajectories

Joint-space cubic and quintic polynomial trajectories were implemented. Quintic trajectories ensure continuity of position, velocity, and acceleration, resulting in smooth motion suitable for control.

13.2 Task-Space Trajectories (Screw Approach)

For screw assembly, task-space trajectories are particularly important during the approach and insertion phase. The robot may use a straight-line approach along the tool axis while maintaining constant orientation to keep the screwdriver aligned with the screw.

13.3 Trajectory Constraints

Trajectory planning must respect:

- joint limits and actuator saturation,
- velocity/acceleration limits,
- avoidance of singular configurations,
- approach-direction constraints for safe insertion.

13.4 Discussion of Chosen Method

Joint-space trajectories are simple to generate and execute, while task-space trajectories offer better control over tool alignment during insertion. For screw assembly, task-space constraints are most critical near contact.

14 Control

Joint-space PD control and computed-torque control were implemented. The computed-torque controller uses inverse dynamics to cancel nonlinear robot dynamics, yielding near-linear closed-loop behavior.

For screw assembly, task-space accuracy is more critical than joint-space accuracy. Small orientation errors at the tool tip can lead to cross-threading or failure of assembly. Therefore, controller performance is evaluated in task space, particularly in terms of end-effector orientation alignment and smooth approach along the tool axis.

14.1 Force/Torque Considerations (Extension)

Although explicit force control is not implemented here, screw assembly is inherently an interaction task. Future work may include hybrid position–force control or torque control about the tool axis to regulate tightening torque and axial insertion force.

15 Conclusion

15.1 Overall System Evaluation

A complete analytical and numerical model of a 6-DOF serial screw assembly robot was developed and validated using standard robotics theory. The framework includes kinematics, Jacobian-based analysis, statics, dynamics, trajectory generation, and control.

15.2 Summary of Results

- MDH-based forward kinematics and Jacobian formulations were derived and verified numerically.
- Workspace sampling and manipulability analysis identified singular configurations relevant to tool orientation control.
- Static torque mapping using J^T was formulated for assembly wrenches.
- Recursive Newton–Euler dynamics were implemented for joint torque prediction.
- Smooth joint-space (cubic/quintic) trajectories were generated and evaluated for control.

15.3 Suitability for Intended Application

The 6R serial manipulator architecture is well suited for screw assembly tasks requiring precise position and orientation control. The availability of full rotational freedom enables reliable alignment with threaded features and supports consistent fastening operations.

15.4 Final Design Justification

Compared to simpler Cartesian or SCARA robots, the selected 6R structure provides the necessary dexterity and orientation capability required for screw assembly. Although mechanically more complex, this configuration is justified by the task requirements and represents an appropriate and effective robotic solution.

15.5 Recommendations

Recommended future improvements include (i) explicit tool torque/axial force control, (ii) improved calibration of the tool frame T_6^E, and (iii) collision-aware trajectory planning in a realistic workcell with fixtures and feeders.

A Symbolic Forward Kinematics

The complete symbolic forward kinematics of the manipulator were derived using the Modified Denavit–Hartenberg convention. The end-effector pose is given by:

$$T_0^6 = A_1 A_2 A_3 A_4 A_5 A_6. \tag{11}$$

The resulting homogeneous transformation matrix is:

$$T_0^6 = \begin{bmatrix} r_{11} & r_{12} & r_{13} & p_x \\ r_{21} & r_{22} & r_{23} & p_y \\ r_{31} & r_{32} & r_{33} & p_z \\ 0 & 0 & 0 & 1 \end{bmatrix}, \tag{12}$$

where the elements r_{ij} and p_x, p_y, p_z are functions of the joint variables $\theta_1, \ldots, \theta_6$.

B Geometric Jacobian Derivation

The geometric Jacobian was derived from the forward kinematics by differentiating the end-effector position and orientation with respect to the joint variables. For a serial manipulator with revolute joints, the Jacobian columns are defined as:

$$J_{v,i} = z_{i-1} \times (p_6 - p_{i-1}), \quad J_{\omega,i} = z_{i-1}. \tag{13}$$

The full Jacobian matrix is given by:

$$J(q) = \begin{bmatrix} J_v(q) \\ J_\omega(q) \end{bmatrix}. \tag{14}$$

The symbolic Jacobian was verified numerically using finite-difference approximations of the end-effector velocity.

C Analytical Inverse Kinematics Derivation

The inverse kinematics problem was solved analytically by decoupling position and orientation. The wrist center position is computed as:

$$p_w = p_0^6 - d_6 \hat{z}_6. \tag{15}$$

The first three joint variables are obtained using geometric relations in the plane defined by the first three links. The remaining joints are computed from the relative rotation matrix:

$$R_3^6 = (R_0^3)^T R_0^6. \tag{16}$$

Multiple inverse kinematic solutions exist due to elbow-up/elbow-down and wrist flip configurations.

References

[1] J. J. Craig, *Introduction to Robotics: Mechanics and Control*, 3rd ed., Pearson, 2005.